ISSN 0005–1144
ATKAAF 43(3–4), 119–129 (2002)

Stjepan Bogdan, Zdenko Kovačić

Fuzzy Rule-Based Adaptive Force Control of Single DOF Servo Mechanisms

UDK 62-526
004.896
IFAC IA 5.9.3;4.6.2

Preliminary communication

The paper presents position/force control with a completely fuzzified adaptive force control system for the single degree of freedom servo mechanisms. The proposed force control scheme contains an adaptive fuzzy force controller and a subordinated fuzzy velocity controller. By using a second-order reference model, a model reference--based fuzzy adaptation mechanism is able to keep the error between the model and system output responses within desired limits. The results obtained by computer simulations indicate a stable performance of the force control system for a wide range of environment stiffness variations. The proposed adaptive force control method has also been effective in case of a contact with a rough surface or a complex form workpiece.

Key words: force/position control, fuzzy logic control algorithms, adaptive control

1 INTRODUCTION

Most of the presently used machine tools and manipulators are designed as position and orientation controlled mechanisms. If a mechanism is only position controlled, then execution of some operations such as the edge following of complex form workpiece may become a problem. In case that the surface of the manipulated workpiece is very rough, then position control also becomes ineffective. Another problem results from progressive wear of the abrasive tool. In that case, it is very difficult to maintain the constant contact force and eventually, the tool can loose or lose the contact with the workpiece.

Force control systems have been developed to solve these problems. A number of papers deal with different techniques of force control applied mostly to robotic mechanisms (manipulators). In spite of some specific approaches as position/force control via sensor programming [1, 2], discontinuous control [3] or joint torque control [4, 5], most of the control schemes could be divided into two groups:

1) hybrid position/force control,
2) impedance control.

Hybrid position/force control includes independent force and position control. Force control takes place on the hyper plane normal to the constraint surface and position/velocity control occurs on the tangential hyper plane [6, 7, 8, 9]. Simultaneous stabilization of both desired robot motion and the desired interaction force is described in [10]. The inverse dynamics approach for robot control applied to redundant robots with rigid or flexible joints can be used for the synthesis of a robust position/force controller [11]. The inverse dynamics approach may also result in the efficient learning method for motion and force control [12].

Impedance control is a general concept which considers dynamic interaction of two physical systems as interaction of impedance and admittance. Controlled stiffness methods have most frequently been developed [13, 14], but they can face the problem of instability of the impedance-controlled manipulator in case of contact with the different stiffness environment. In [15, 16] authors addressed dynamic problems in force control caused by mechanical properties of a robot mechanism.

A model reference-based adaptive control scheme, which estimates unknown stiffness of the environment, has been developed [17, 18]. Another scheme is based on estimation of unknown parameters by measurement of position, velocity and acceleration [19]. Estimation of unknown stiffness has been accomplished by using dual force sensor, passive and active, which allows estimation of the contact position and the environment stiffness simultaneously [20].

Force control encounters the problem of poorly known environment parameters, which in turn represents an ideal case for introduction of model-independent control techniques such as those based on the usage of a fuzzy logic [21, 22]. A fuzzy predictive algorithm can increase effectiveness of a classical impedance controller when they work in parallel [23]. Efficient adjustment strategies can be

developed for a fuzzy-neuro force controller using genetic algorithms to deal with robot force control in an unknown environment [24].

This paper shows the benefits of introducing a fuzzy logic into adaptive contact force control. Instead of complex estimation and control algorithms, a simple fuzzy-rule based adaptive control scheme has been developed, which significantly decreases the computational time and does not require excessive hardware. For performance evaluation, the proposed force control method has been applied to a single degree of freedom servo mechanism. A studied control system consists of the outer explicit force control loop and the inner velocity control loop. The velocity control loop contains a fuzzy controller, and the force control loop contains a fuzzy controller with a fuzzy model reference-based algorithm for tuning of the fuzzy force controller output. A permanent magnet synchronous motor (PMSM) has been used to drive the studied servo mechanism. The results obtained by computer simulations indicate a stable performance of the force control system for a wide range of environment stiffness variations. Moreover, the proposed adaptive force control method has satisfactorily performed in case of contact with the rough surface or in case of edge following of the complex form workpiece.

2 DESCRIPTION OF THE SYSTEM

A single degree of freedom mechanism considered for adaptive force control during a contact with the environment is shown in Figure 1. A contact force is measured by the force sensor. The mechanism is normally position controlled, except during the contact when it is force controlled.

The mechanism is driven by a vector controlled chopper-fed PMSM whose control characteristics are similar to those of a DC motor. An angular speed control loop shown in Figure 2 contains a PI controller with $U_{r\omega}$ as a reference input and $U_{r\omega}$ as a speed feedback signal. Thanks to the applied vector control concept, a motor torque T_e is proportional to the q-component of the stator current i_q, while the current control loop is represented by a first order transfer function (gain K_{cc} and time constant T_{cc}). The rated parameter values of a linearized model of the velocity control system (Figure 2) were as follows: $T_s = 0.5$ ms, $K_{cc} = 1$ A/V, $T_{cc} = 50$ μs, $K = 0.9837$ Vs, $J_T = 0.00176$ kgm^2, $B = 0.000388$ Nms, $T_M = J_T/B = 4.536$ s, $K_\omega = 0.063$ Vs, $T_\omega = 0.0025$ s.

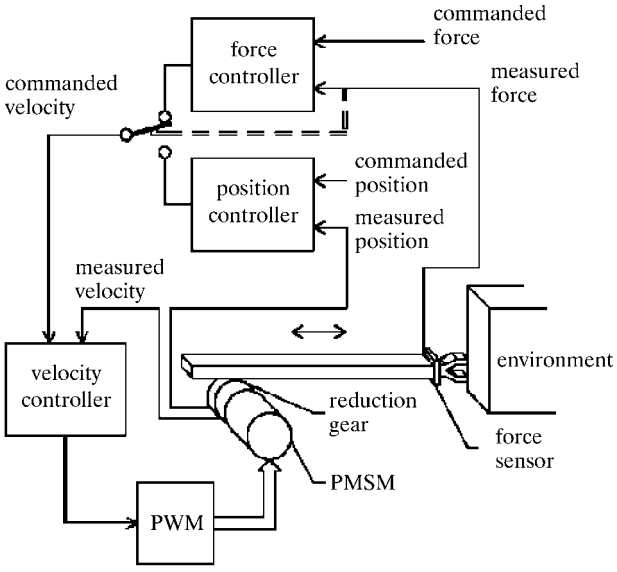

Fig. 1 Force control system of a one DOF manipulator

For the system shown in Figure 1 a model used for the contact description was built as shown in Figure 3.

It is described with the following differential equations

$$m_1\ddot{x}_1 + b_s(\dot{x}_1 - \dot{x}_2) + K_s(x_1 - x_2) = F, \quad (1)$$

$$m_2\ddot{x}_2 + b_s(\dot{x}_2 - \dot{x}_1) + K_s(x_2 - x_1) + K_e(x_2 - x_3) = 0, \quad (2)$$

$$T = F \cdot r,\ \dot{x}_1 = v_1,\ \dot{x}_2 = v_2,\ v_1 = \omega \cdot r, \quad (3)$$

where m_1 mass of a manipulator (without end effector), kg,

m_2 mass of end effector, kg,

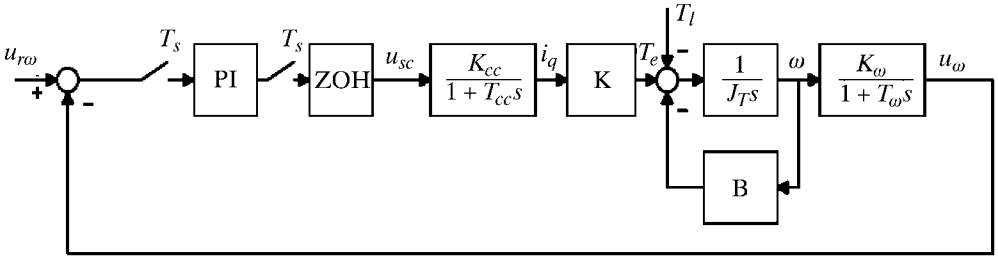

Fig. 2 Linearized model of a PMSM angular speed control system

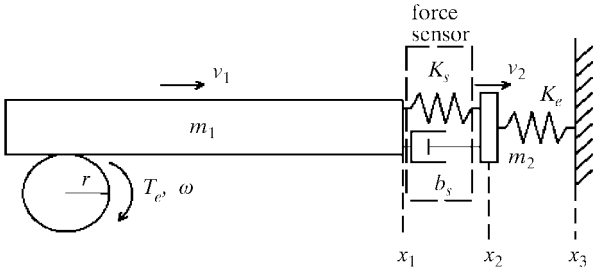

Fig. 3 Model of a contact between the manipulator and the environment

x_1 position of a manipulator, m,
x_2 position of end effector, m,
x_3 position of workpiece in contact with end effector, m,
v_1 velocity of a manipulator, m/s,
v_2 velocity of end effector, m/s,
ω angular velocity of a motor, rad/s,
b_s, K_s damping and stiffness coefficients of a force sensor,
K_e stiffness coefficient of environment, N/m,
F force applied to a manipulator, N,
T torque needed to produce force F, Nm,
r radius of reduction gear, m.

Torque equation has a form:

$$T_e = J_T\dot{\omega} + B\omega + T. \tag{4}$$

On inserting equations (3) and (4) into equations (1) and (2), we obtain

$$\dot{v}_1 = \frac{1}{J_e}\left[T_e - B_e v_1 + rb_s v_2 - rK_s(x_1 - x_2)\right], \tag{5}$$

$$\dot{v}_2 = \frac{1}{m_2}\left[b_s v_1 - b_s v_2 + K_s(x_1 - x_2) - K_e(x_2 - x_3)\right], \tag{6}$$

where

$$J_e = \frac{J_T}{r} + rm_1,\ B_e = \frac{B}{r} + rb_s.$$

Equations (5) and (6) include a term $K_s(x_1 - x_2)$ describing the stiffness force component detected by a force sensor and term $K_e(x_2 - x_3)$ describing the contact force between the end effector and the workpiece. The force detected by the force sensor is used as a feedback signal and besides the stiffness component it also contains a damping component $b_s(v_1 - v_2)$. In the studied control system, the variable x_3 is acting as a disturbance which may be caused by the rough surface or by the complex form of the workpiece.

3 A SYNTHESIS OF VELOCITY AND FORCE CONTROLLERS

A synthesis of the velocity control loop is performed under assumption of the unconstrained motion of the mechanism, as it was a position-controlled mechanism. In this case, terms in equations (5) and (6) caused by the contact disappear. Masses of manipulator and end effector m_1, m_2 together with the manipulator viscous friction coefficient b are substituted with equivalent values referred to the motor shaft. Therefore, J_T should be replaced by $J_T + r^2(m_1 + m_2)$, and B with $B + r^2 b$.

Open-loop transfer function of the linearized PMSM angular velocity control system has a form

$$G_{o\omega}(s) = \frac{K_o(1 + T_{sc}s)}{s(1 + T_{cc}s)(1 + T_M s)(1 + T_\omega s)} \tag{7}$$

where $K_o = K_{sc}K_{cc}KK_MK_T/T_{sc}$ open-loop gain,
$K_M = 1/(B + r^2 b)$ PMSM gain,
$T_M = [J_T + r^2(m_1 + m_2)]/(B + r^2 b)$ PMSM time constant.

In case of $m_1 = 10$ kg, $m_2 = 1$ kg, $r = 0.02$ m and $b = 5$ Ns/m, we obtain $K_M = 418.76$, $T_M = 2.579$ s, $K_o = 26.254$. The PI velocity controller parameters provided the desired root loci: $K_{sc} = 15$ and $T_{sc} = 0.03$ s. In that case the response of the angular velocity feedback signal had an overshoot of 20 % (Figure 4).

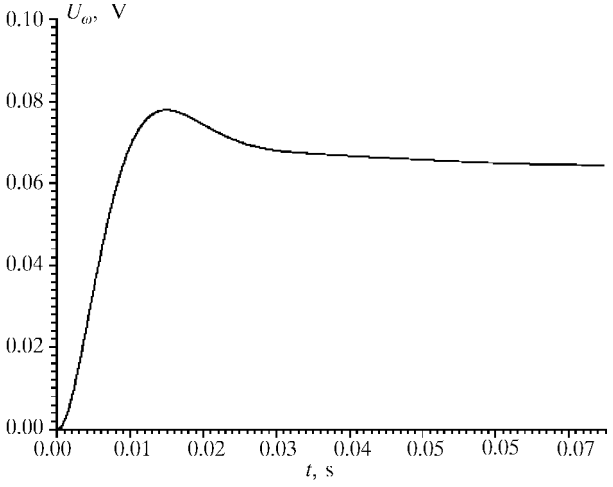

Fig. 4 The response of the velocity feedback signal with a PI velocity controller

The difference between the commanded velocity and the velocity feedback signal is related to the motor torque in the following way

$$G_1(s) = \frac{T_e(s)}{e_\omega(s)} = K_{sc}\frac{1 + T_{sc}s}{T_{sc}s}K\frac{K_{cc}}{1 + T_{cc}s}. \tag{8}$$

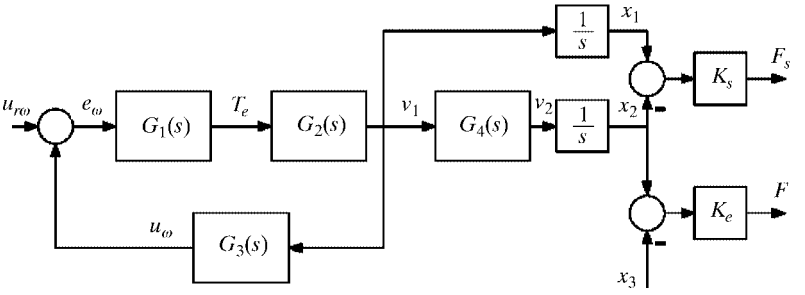

Fig. 5 Open-loop force control system (without a force controller)

Let us now assume that $x_3 = 0$ (no changes in the workpiece profile). If we transform equations (5) and (6) by using the Laplace transformation, we obtain the transfer function which describes the relation between the manipulator velocity and the motor torque:

$$G_2(s) = \frac{v_1(s)}{T_e(s)} = \frac{s(m_2 s^2 + b_s s + K_e + K_s)}{a_4 s^4 + a_3 s^3 + a_2 s^2 + a_1 s + a_0} \tag{9}$$

where

$$a_0 = rK_s K_e,\ a_1 = K_s(B_e - rb_s) + B_e K_e,$$
$$a_2 = K_s(J_e + rm_2) + b_s(B_e - rb_s) + J_e K_e,$$
$$a_3 = J_e b_s + B_e m_2,\ a_4 = J_e m_2.$$

A velocity feedback transfer function is defined by

$$G_3(s) = \frac{u_\omega(s)}{v_1(s)} = \frac{K_\omega}{r(1 + T_\omega s)}. \tag{10}$$

Relation between the manipulator and the end effector velocities is described by the following transfer function

$$G_4(s) = \frac{v_2(s)}{v_1(s)} = \frac{b_s s + K_s}{m_2 s^2 + b_s s + K_s + K_e}. \tag{11}$$

Finally, the transfer function of the open-loop force control system without a force controller (Figure 5) has a form

$$G_{oF}(s) = \frac{F_s(s)}{u_{r\omega}(s)} =$$

$$= K_s\left[1 - G_4(s)\right]\frac{1}{s}\frac{\left[G_1(s)G_2(s)\right]}{1 + G_1(s)G_2(s)G_3(s)}. \tag{12}$$

On inserting (8), (9), (10) and (11) into (12), we obtain

$$G_{oF}(s) = \frac{KK_s K_{cc} K_{sc}(1 + T_{sc}s)(1 + T_\omega s)(m_2 s^2 + K_e)}{T_{sc}s(b_6 s^6 + b_5 s^5 + b_4 s^4 + b_3 s^3 + b_2 s^2 + b_1 s + b_0)} \tag{13}$$

where

$$b_0 = a_0 + K_2(K_s + K_e),$$
$$b_1 = a_1 + a_0(T_{cc} + T_\omega) + K_2\left[b_s + (K_s + K_e)T_{sc}\right],$$
$$b_2 = a_2 + a_1(T_{cc} + T_\omega) + a_0 T_{cc} T_\omega + K_2(m_2 + b_s T_{sc}),$$
$$b_3 = a_3 + a_2(T_{cc} + T_\omega) + a_1 T_{cc} T_\omega + K_2 m_2 T_{sc},$$
$$b_4 = a_4 + a_3(T_{cc} + T_\omega) + a_2 T_{cc} T_\omega,$$
$$b_5 = a_4(T_{cc} + T_\omega) + a_3 T_{cc} T_\omega,$$
$$b_6 = a_4 T_{cc} T_{\omega,}$$
$$K_2 = \frac{K_{sc} K_\omega K_{cc} K}{T_{sc} r}.$$

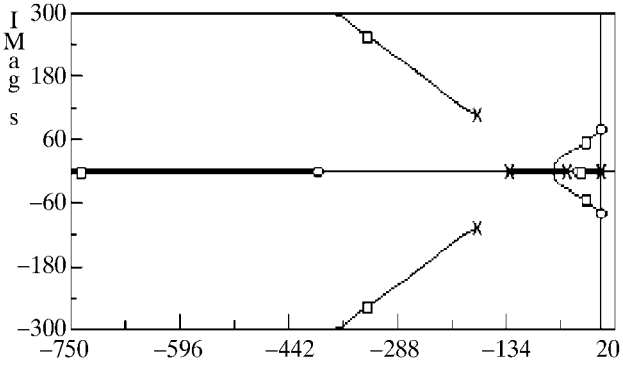

Fig. 6 Force control loop root loci plot for the rubber surface

We choose a proportional force compensator with the gain coefficient K_F. A root loci plot for the equation (13) in case of $b_s = 1000$ Ns/m, $K_s = 100000$ N/m and $K_e = 6000$ N/m (rubber surface) is shown in Figure 6 (zeros = o and poles = x). The closed loop system poles for $K_F = 0.025$ are marked with rectangles.

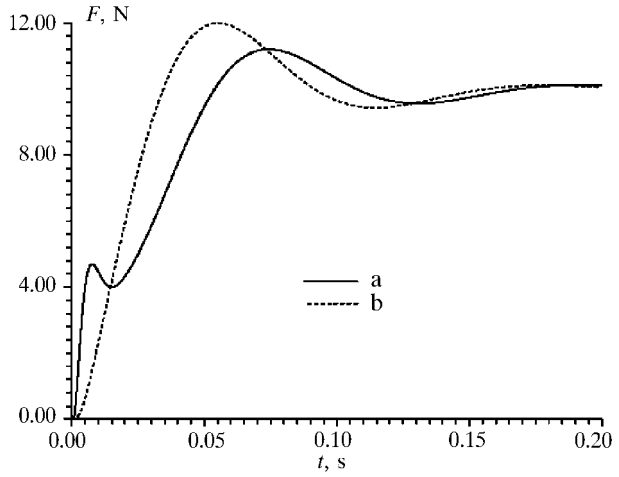

Fig. 7 The responses of the force feedback signal (a) and the contact force (b) (rubber)

The responses of the force feedback signal and the contact force are shown in Figure 7. Due to the presence of the dominant real pole in the vicinity of the phase plane origin, the output of the force sensor has a non-monotonous form. As may be seen, overshoot in the contact force response is approximately 20 % with the time of maximum of 50 ms. Both signals have the same steady-state value of 10 N.

When the stiffness of the environment varies, as in case of contact with the aluminum surface (K_e = = 60000), system dynamics vary too (Figure 8).

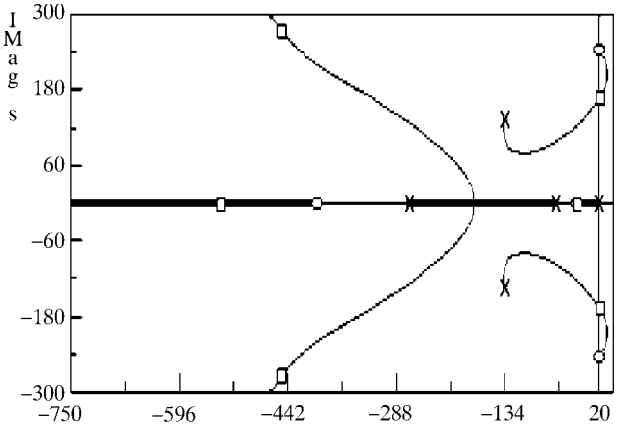

Fig. 8 Force control loop root loci plot for the aluminum surface

In case of $K_F = 0.025$ (force controller gain specified for the rubber surface), poles of the closed--loop force control system (rectangles) are placed in the right-hand side of the *s*-plane, and the contact force response becomes unstable, as shown in Figure 9.

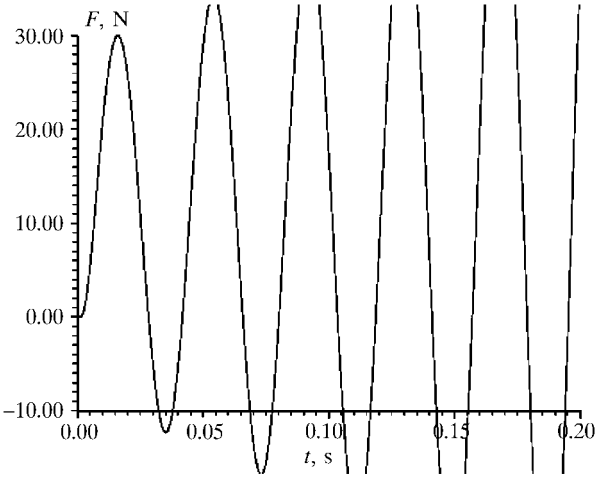

Fig. 9 The contact force response in case of contact with the aluminum surface

4 A SYNTHESIS OF FUZZY VELOCITY AND FORCE CONTROLLERS

A fuzzy velocity controller, which has the error signal $e_\omega(k)$ and the change in error signal $\mathrm{d}e_\omega(k)$ for its inputs, should provide the same quality of the velocity response as it was obtained with a PI controller (Figure 4). To achieve this, seven linguistic subsets are defined for both controller inputs (universes of discourse E and DE): large negative (LN), large positive (LP), medium negative (MN),

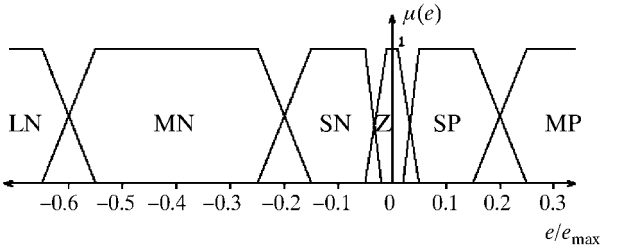

Fig. 10 Distribution of membership functions for $e_\omega(k)$

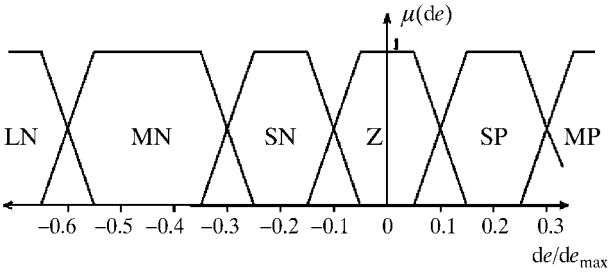

Fig 11 Distribution of membership functions for $\mathrm{d}e_\omega(k)$

medium positive (MP), small negative (SN), small positive (SP), and zero (Z). In the studied case the maximum change of commanded velocity was estimated to be 0.3, and therefore the maximum error value was $-0.3 \le e_\omega \le 0.3$. The maximum error change during the control interval $T_s = 0.5$ ms was estimated to be $-0.04 \le \mathrm{d}e_\omega \le 0.04$. The distribution of membership functions along e and de axes are shown in Figures 10 and 11, respectively.

Values of the centroid (singletons) in the inference table have been heuristically determined and their graphical presentation is shown in Figure 12. The membership functions $\mu(e_\omega)$ and $\mu(\mathrm{d}e_\omega)$, always referring to a set of four out of forty-nine possible IF-THEN control rules, define the fuzzy control surface and consequent fuzzy controller output by following the centre of gravity principle [25].

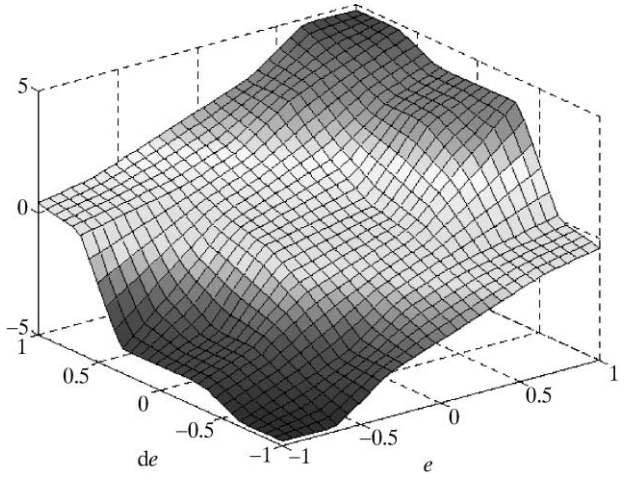

Fig. 12 The control surface of the fuzzy angular velocity controller

The fuzzy velocity controller is changing modes of operation depending on the magnitudes of its inputs, error $e_\omega(k)$ and change in error $\mathrm{d}e_\omega(k)$, according to the following set of relations:

$$\begin{aligned} &e_\omega(k) \in \textbf{ZE} \;\&\; \mathrm{d}e_\omega(k) \in \textbf{ZDE} \Rightarrow \textbf{INTEGRAL MODE} \\ &e_\omega(k) \notin \textbf{ZE} \;\&\; \mathrm{d}e_\omega(k) \notin \textbf{ZDE} \Rightarrow \textbf{NONINTEGRAL MODE} \end{aligned} \tag{14}$$

The fuzzy velocity controller operates in the integral mode of operation

$$u_{sc}(k) = u_{sc}(k-1) + K_i \Delta u_{sc}(k) \tag{15}$$

to support the steady state accuracy and compensate for the disturbance effects. In case of large changes of the reference input, the fuzzy controller operates in the nonintegral mode.

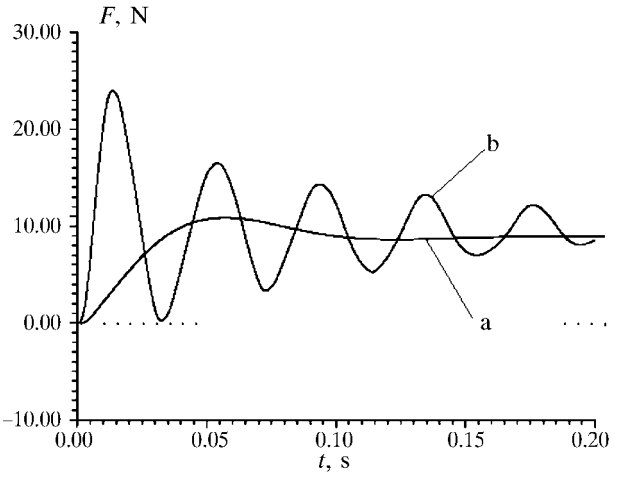

Fig. 13 The contact force response with fuzzy velocity controller and P force compensator in case of contact with rubber (a) and aluminum (b) surface

With so designed fuzzy velocity controller the contact force response in case of contact with the rubber surface has a form as shown in Figure 13(a). If compared with the contact force response shown in Figure 7, the difference between them is negligible.

The contact force response obtained with the fuzzy velocity controller in case of contact with the aluminum surface is shown in Figure 13(b). Despite noticeable oscillations in response, we have obtained a stable force response. Compared to the unstable response obtained with the PI velocity controller (Figure 9), it may be seen that the fuzzy velocity controller contributes to the stabilization of a system.

Further improvement can be achieved by using a fuzzy control algorithm in the force control loop. Let us use the same type of algorithm, which will be designed for the contact with the rubber surface. The maximum change of the commanded force was estimated to be 10 N, and therefore the maximum error value was $-10.0 \le e_F \le 10.0$. The maximum error change during the control interval $T_s = 0.5$ ms was estimated to be $-0.7 \le \mathrm{d}e_F \le 0.7$. The distribution of membership functions along e and de axes is the same as with the fuzzy velocity controller (Figures 10 and 11). The force controller output value is also defined by following the centre of gravity principle. The inference table has been organized in the same manner as with the velocity controller (Figure 12). Only a scaling of the centroid in the fuzzy rule table (division by 20) has been done to obtain the desired contact force performance.

Figure 14(a) shows the response of the contact force in case of contact with the rubber surface when both controllers are fuzzy. Overshoot and

time of maximum are almost the same as they were in case of using standard controllers (Figure 7). In case of contact with the aluminum surface, the contact force response has a form as shown in Figure 14(b).

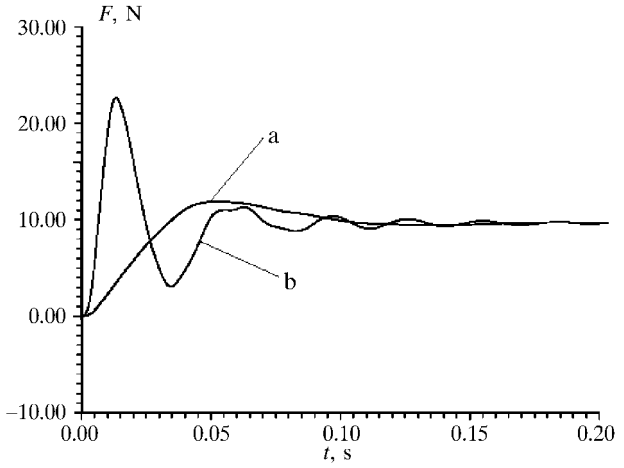

Fig. 14 The contact force response with fuzzy force and velocity controllers in case of contact with rubber (a) and aluminum (b) surface

As may be seen, introduction of the fuzzy controller into the force control loop has further stabilized the system response. Sensitivity to environment stiffness variations has been noticeably reduced, but there is still a problem of the first maximum which is too high. We have tried to solve the problem by developing appropriate algorithm for tuning of the fuzzy force controller output which would ensure almost the uniform contact force response in case of contact with varying stiffness environment.

5 FUZZY LOGIC-BASED TUNING OF THE FUZZY FORCE CONTROLLER OUTPUT

The proposed adaptive force control scheme is shown in Figure 15. It is composed of the fuzzy force controller and a model reference-based fuzzy algorithm for tuning of the fuzzy force controller output.

The reference model has been taken as a model of a second-order system

$$G_{FM} = \frac{U_{FM}(s)}{U_{rF}(s)} = \frac{\omega_0^2}{s^2 + 2\zeta_0\omega_0 s + \omega_0^2}, \qquad (16)$$

where a damping coefficient ζ_0 and a natural frequency ω_0, [rad], are defined by performance indices such as an overshoot σ_m and a time of maximum t_m of the force feedback response. It must be noted that the parameters ζ_0 and ω_0 are referred to the contact with the rubber surface. The force feedback response, shown in Figure 6, had the overshoot in response of $\sigma_m = 10$ % and time of maximum was $t_m = 0.075$ s. This has yielded: $\zeta_0 = 0.6$ and $\omega_0 = 52.36$ rad/s. The response of the reference model is shown together with the force feedback response in Figure 16.

The main goal of a fuzzy adaptation mechanism design was to create such a group of fuzzy control rules which would permanently issue tuning coefficient values required for adaptation of the fuzzy force controller output, in order to get the contact force transient response unaffected by variations of the environment. In the proposed control scheme shown in Figure 15, an adapted force controller output is given by

$$u_{r\omega} = K_A u_{Fc}, \qquad (17)$$

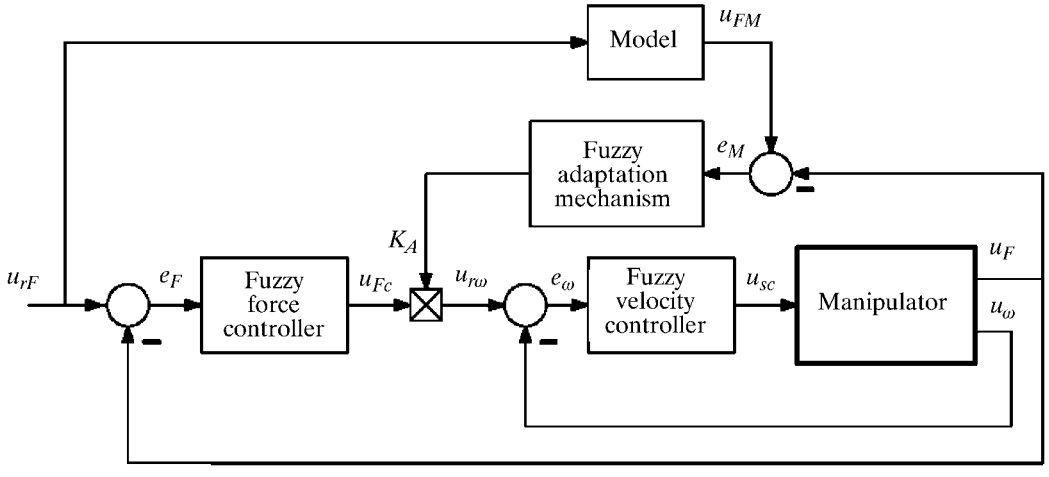

Fig. 15 Fuzzy model reference-based adaptive force control system

where $u_{r\omega}$ is the adapted force controller output (reference velocity), K_A is the tuning coefficient and u_{Fc} is the force controller output. Such a concept assumes that the steady state tuning coefficient value is equal to one.

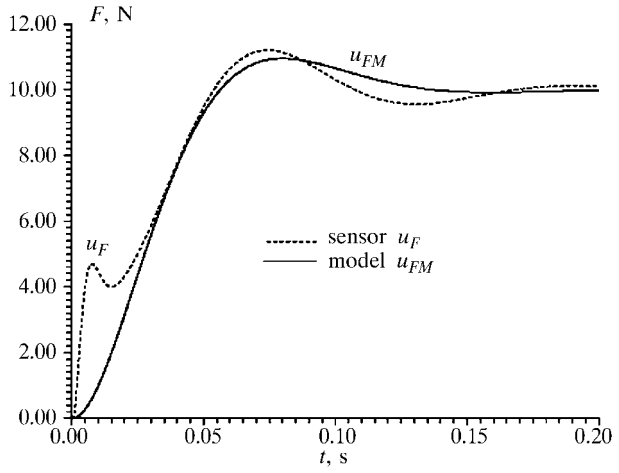

Fig. 16 The responses of the reference model and the force feedback signal in case of contact with the rubber surface

The developed fuzzy adaptation algorithm has a nonintegral character, i.e. the current tuning coefficient value does not depend on the previous values. In this way, the magnitude of the tuning coefficient is directly determined by the magnitudes of the inputs. The inputs of the fuzzy adaptation algorithm (Figure 15) are defined by the following equations

$$e_M(k) = u_{FM}(k) - u_F(k), \tag{18}$$

$$\mathrm{d}e_M(k) = e_M(k) - e_M(k-1), \tag{19}$$

where $u_F(k)$ is the force feedback signal, and $u_{FM}(k)$ is the reference model output (desired force feedback).

A fuzzy adaptation mechanism has also seven linguistic subsets defined for both inputs (universes of discourse E and DE): LN, LP, MN, MP, SN, SP, and Z. For the studied force control system the maximum error value was estimated to be 2.5, i.e. $-2.5 \le e_M(k) \le 2.5$. The maximum error change during the control interval $T_s = 0.5$ ms was estimated to be 0.75, i.e. $-0.75 \le \mathrm{d}e_M(k) \le 0.75$. The distributions of membership functions along e_M and $\mathrm{d}e_M$ axes are shown in Figure 17.

The size of fuzzy subsets and centroid values were defined in order to keep the tracking error e_M within 20 % of the imposed change of the reference input:

$$|e_M| \le 0.2\,\Delta u_r. \tag{20}$$

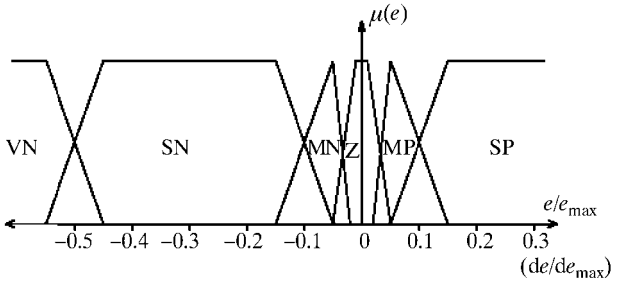

Fig. 17 The distributions of membership functions for both inputs of the fuzzy adaptation mechanism

The values of centroid in the fuzzy rule table of the discussed adaptation mechanism are defined as shown in Table 1. The adaptation mechanism output, i.e. the tuning coefficient K_A, is also obtained by following the centre of gravity principle.

Table 1 **The centroid values of the adaptation mechanism**

	LNE	MNE	SNE	ZE	SPE	MPE	LPE
LNDE	–1.0	–1.0	–1.0	–0.5	0.75	0.9	1.0
MNDE	–1.0	–0.5	–0.25	0	0.9	1.0	1.1
SNDE	–1.0	–0.25	–0.25	0.25	1.0	1.1	1.15
ZDE	–0.5	0	0.5	1.0	1.1	1.15	1.3
SPDE	0.5	0.75	1.0	1.1	1.15	1.3	2.0
MPDE	0.9	1.0	1.1	1.15	1.3	1.5	2.0
LPDE	1.0	1.1	1.15	1.3	2.0	2.0	2.0

Figure 18 shows the contact force responses in case of a contact with the rubber ($K_e = 6000$) and aluminum ($Ke = 60000$) surfaces. Figure 19 shows

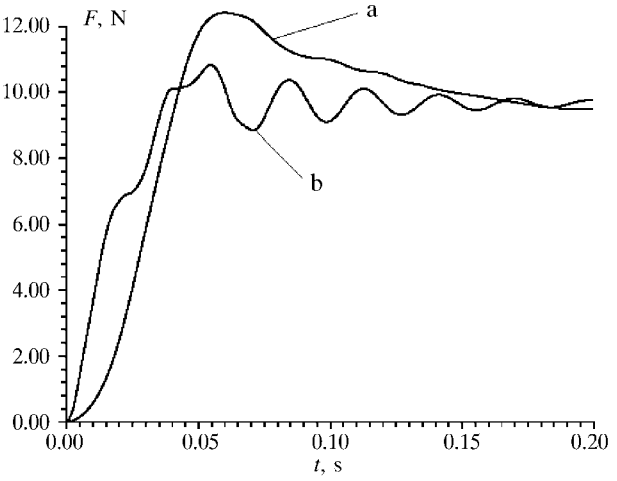

Fig. 18 The contact force response with adaptive force controller in case of contact with the rubber (a) and aluminum (b) surface

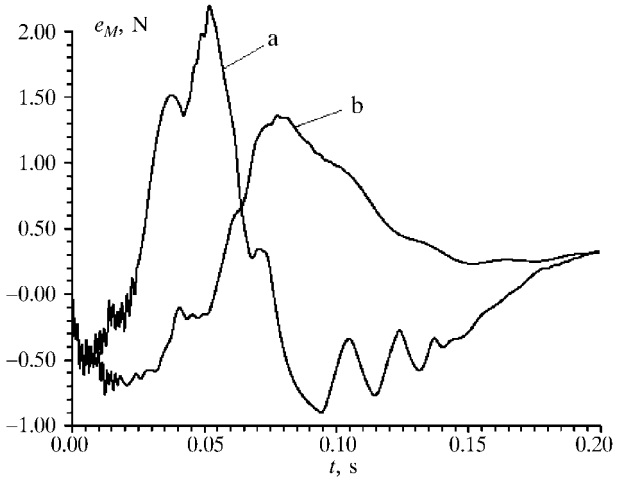

Fig. 19 The tracking error response with adaptive force controller in case of contact with the rubber (a) and aluminum (b) surface

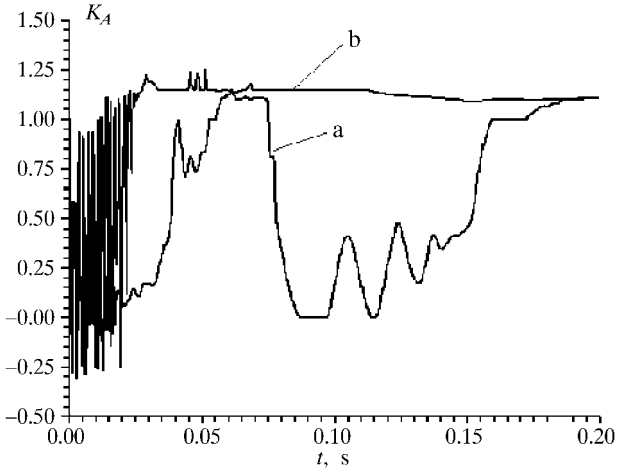

Fig. 20 The tuning coefficient response in case of contact with rubber (a) and aluminum (b) surface

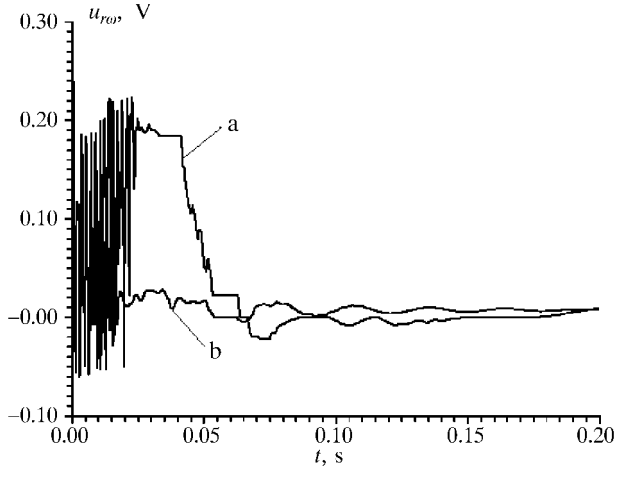

Fig. 21 The adapted force controller output response in case of contact with the rubber (a) and aluminum (b) surface

the tracking error responses, Figure 20 shows the tuning coefficient responses and Figure 21 shows the adapted force controller output responses for both cases.

The tuning coefficient is oscillatory in the initial part of the response as the fuzzy-logic tuning algorithm attempts to compensate for the non-monotonous character of the force feedback sensor response (see Figures 7 and 16). The tracking error is kept within ± 20 % of the imposed change of the reference force input (10 N), thus proving a good adaptation in case of varying environment stiffness. Since the reference model is a second-order system and the studied force control system is the seventh--order system, the simulation results have shown that fuzzy logic has achieved what could not be expected to achieve with standard model reference--based methods of adaptive control. The experiments have included a contact with the rubber and aluminum surface, thus showing the ability of the force-controlled mechanism to successfully manipulate the workpiece made of different materials.

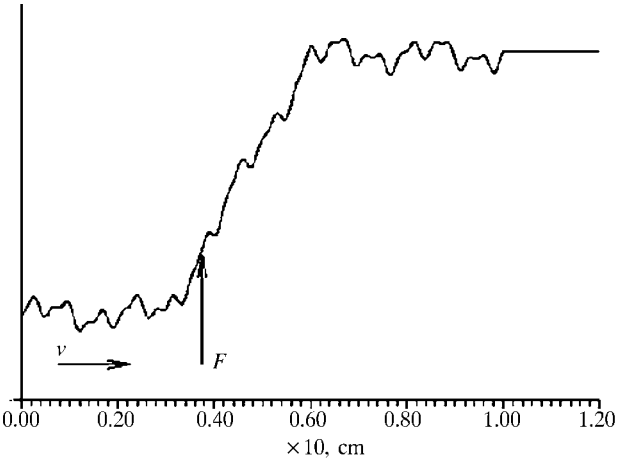

Fig. 22 The profile of the manipulated workpiece

Let us now suppose that the manipulator follows the edge of a workpiece with a complex profile, as shown in Figure 22. The tool travels along the ordinate axis to the right with velocity of 10 cm/s and simultaneously acts on the workpiece with the constant contact force of 10 N. In the studied force control system, such a task may be described as a test of system's ability to act in the presence of disturbance x_3 (Figure 5).

Figure 23 shows the difference between the reference force value (10 N) and the actual contact force in case of using standard (a) and adaptive fuzzy controllers (b) for the contact with the rubber surface. In both cases the difference is kept below 5 % of the given force value.

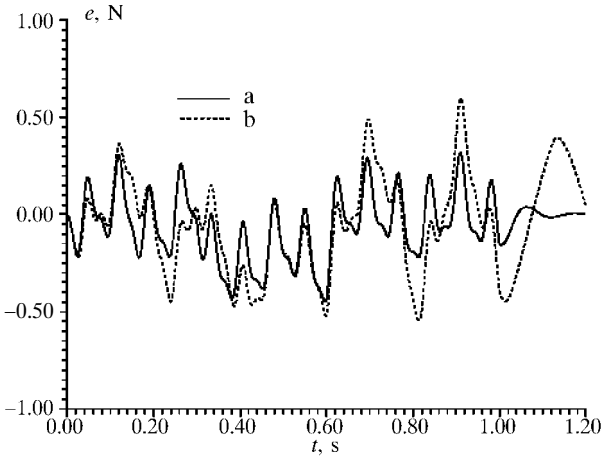

Fig. 23 The force error response in case of contact with the rubber surface: profile following with standard force compensators (a) and adaptive fuzzy compensators (b)

But if the mechanism is in contact with the aluminum surface (Figure 24), adaptive control scheme shows superior performance, because system with standard controllers has become unstable, and adaptive force controller has stabilized the system holding the difference within 30 % of the given force value.

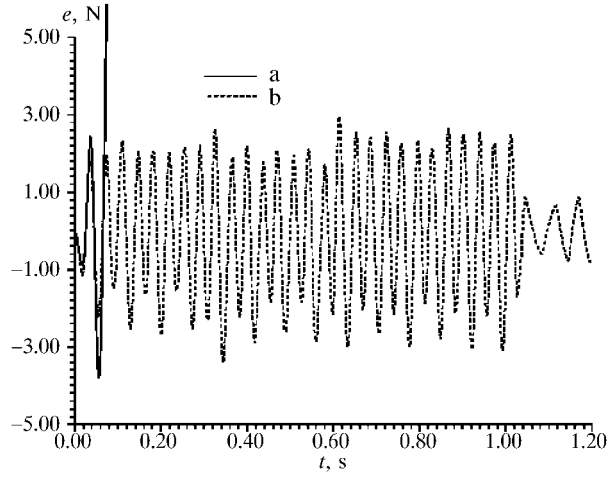

Fig. 24 The force error response in case of contact with the aluminum surface: profile following with standard force compensators (a) and adaptive fuzzy compensators (b)

According to the simulation results, the proposed adaptive force control method has satisfactorily performed even in case of active disturbance caused by the complex workpiece profile or the very rough surface.

6 CONCLUSIONS

We have presented a completely fuzzified adaptive force control scheme developed for the single degree of freedom servo mechanisms. The force control loop contains an adaptive fuzzy force controller and a subordinated fuzzy velocity controller. A model reference-based fuzzy adaptation algorithm has been used for tuning of the fuzzy force controller output. The adaptation algorithm has a nonintegral character and it is active only during the system transitions, since the tuning coefficient assumes the unity value before and after the transient response. A stand-by position during a steady-state makes it permanently ready for action.

Effectiveness of the proposed adaptive force control scheme has been tested by computer simulation experiments in case of a varying stiffness of the environment. The studied force control system has been modelled as a seventh-order system. By using a second-order reference model, the error between the model and the system output responses has been successfully maintained within the desired limits for a wide range of environment stiffness variations (rubber, aluminum).

The simulation results have also indicated a good performance of the force control system in case of active disturbance caused by the complex workpiece profile or the very rough surface.

Even though the proposed fuzzy control scheme stabilizes the system in case of environment parameter variations, a heuristic nature of its design makes a rigorous stability analysis very difficult. The stability mainly depends on designer's experience with determination of fuzzy controller parameters.

REFERENCES

[1] G. Hirzinger, J. Heindl, **Sensor Programming – a New Way for Teaching Robot Raths and Forces/Torques Simultaneously.** The Third Int. Conf. on Robot Vision and Sensory Controls, Cambridge, MA, Nov. 1983.

[2] G. Plank, G. Herzinger, **Controlling a Robot's Motion Speed by a Force-torque-sensor for Deburring Problems.** Proc. 4th IFAC/IFIP Symp. Informat. Contr. Probl. in Manuf. Tech., pp. 97–102, Oct. 1982.

[3] J. K. Mills, D. M. Lokhorst, **Stability and Control of Robotic Manipulators During Contact/Noncontact Task Transition.** IEEE Trans. on Rob. and Auto., vol. 9, no. 3, 1993.

[4] J. Y. S. Luh, W. D. Fisher, R. P. C. Paul, **Joint Torque Control by a Direct Feedback for Industrial Robots.** IEEE Trans. Automat. Contr., vol. AC-28, no. 2, pp. 153–161, Feb. 1983.

[5] C. H. Wu, R. P. Paul, **Manipulator Compliance Based on Joint Torque Control.** Proc. 20th IEEE Conf. Decision Contr., vol. 1, pp. 265–270, Dec. 1981.

[6] J. J. Craig, M. H. Raibert, **A Systematic Method of Hybrid Position/Force Control of a Manipulator.** Proc. IEEE Computer Software & Appl. Conf., pp. 446–451, Nov. 1979.

[7] M. H. Raibert, J. J. Craig, **Hybrid Position/Force Control of Manipulators.** IEEE Trans. Syst., Man, Cybern., vol. SMC-II, no. 6, pp. 418–432, June 1981.

[8] T. Yoshikawa, A. Sudou, **Dynamic Hybrid Position/Force Control of Robot Manipulators – On-line Estimation of Unknown Constraint.** IEEE Trans. on Rob. and Auto., vol. 9, no. 2, 1993.

[9] A. A. Goldenberg, P. Song, **Principles for Design of Position and Force Controllers for Robot Manipulators.** Robotics and Autonomous Systems, no. 21, pp. 263–277,1997.

[10] M. Vukobratović, R. Stojić, Y. Ekalo, **Contribution to the Position/Force Control of Manipulation Robots Interacting with Dynamic Environment – A Generalization.** Automatica, vol. 34, No. 10, pp. 1219–1226, 1998.

[11] K. P. Jankowski, H. A. ElMaraghy, **Robust Hybrid Position/ Force Control of Redundant Robots.** Robotics and Autonomous Systems, no. 27, pp. 111–127, 1999.

[12] E. Burdet, L. Rey, A. Codourey, **A Trivial and Effcient Learning Method for Motion and Force Control.** Engineering Applications of Artificial Intelligence, no. 14, pp. 487–496, 2001.

[13] R. Paul, B. Shimano, **Compliance and Control.** Proc. Joint Autom. Contr. Conf., pp. 694–699, 1976.

[14] J. K. Salisbury, **Active Stiffness Control of a Manipulator in Cartesian Coordinates.** Proc. 19th IEEE CDC, vol. 1, pp. 95–100, Dec. 1980.

[15] S. D. Eppinger, W. P. Seering, **Implicit Force Control for Industrial Robots in Contact with Stiff Surfaces.** Automatica, vol. 33, no. 11, pp. 2041–2047, 1997.

[16] P. Rocco, G. Ferretti, G. Magnani, **Three Dynamic Problems in Robot Force Control.** IEEE Trans. on Rob. and Aut., vol. 8, no. 6, 1992.

[17] T. Yabuta, et al., **Force Control of Servomechanism Using Adaptive Control.** IEEE Journal of Rob. and Aut., vol. 4, no. 2, 1988.

[18] S. K. Singh, D. O. Popa, **An Analysis of Some Fundamental Problems in Adaptive Control of Force and Impedance Behavior: Theory and Experiments.** IEEE Trans. on Rob. and Aut., vol. 11, no. 6, 1995.

[19] K. Y. Lian, J. H. Jean, L. C. Fu, **Adaptive Force Control of Single-Link Mechanism with Joint Flexibility.** IEEE Trans. on Rob. and Aut., vol. 7, no. 4, 1991.

[20] B. Nemec, L. Žlajpah, **On Adaptive Control of Force Controlled Manipulators – Implementation and Experimental Results.** Proc. of the 1992 IEEE International Conference on Robotics and Automation, pp. 1882–1888, Nice, 1992.

[21] F. Naghdy, N. P. Nguyen, **Fuzzy Logic Compliance Control of the Peg in Hole Insertion.** Control Engineering Practice, no. 6, pp. 1459–1474, 1998.

[22] L. Huang, S. S. Ge, T. H. Lee, **Fuzzy Unidirectional Force Control of Constrained Robotic Manipulators.** Fuzzy Sets and Systems, 2002.

[23] L. F. Baptista, J. M. Sousa, J. M. G. Sa da Costa, **Fuzzy Predictive Algorithms Applied to Real-Time Force Control.** Control Engineering Practice, no. 9, pp. 411–423, 2001.

[24] K. Kiguchi, K. Watanabe, T. Fukuda, **Generation of Efficient Adjustment Strategies for a Fuzzy-Neuro Force Controller Using Genetic Algorithms – Application to Robot Force Control in an Unknown Environment.** Information Sciences, vol. 145, pp. 113–126, 2002.

[25] Y. F. Li, C. C. Lau, **Development of Fuzzy Algorithms for Servo Systems.** IEEE Cont. Syst. Mag., pp. 65–71, April 1989.

Neizrazito adaptivno upravljanje silom dodira slijednih mehanizama s jednim stupnjem slobode gibanja. Članak prikazuje upravljanje položajem/silom dodira slijednog mehanizma s jednim stupnjem slobode gibanja korištenjem neizrazitog adaptivnog sustava upravljanja silom. Predložena shema upravljanja silom dodira sadrži adaptivni neizraziti regulator sile i podređeni neizraziti regulator brzine vrtnje. Koristeći referentni model drugog reda, neizraziti na modelu zasnovani adaptacijski mehanizam u stanju je držati razliku između odziva modela i odziva sustava u zadanim granicama. Rezultati dobiveni numeričkim simulacijama pokazuju stabilno vladanje sustava upravljanja silom dodira za široki raspon varijacija krutosti okoline. Predložena metoda adaptivnog upravljanja silom se pokazala uspješnom i u slučaju dodira s neravnom površinom ili s radnim predmetom složena oblika.

Ključne riječi: upravljanje položajem/silom, neizraziti algoritmi upravljanja, adaptivno upravljanje

AUTHORS' ADDRESSES:

Doc. dr. sc. Stjepan Bogdan
Sveučilište u Zagrebu, Fakultet elektrotehnike i računarstva
Unska 3, 10000 Zagreb
E-mail: stjepan.bogdan@fer.hr
URL: http://aus-www.rasip.fer.hr/bogdan/index.html

Prof. dr. sc. Zdenko Kovačić
Sveučilište u Zagrebu, Fakultet elektrotehnike i računarstva
Unska 3, 10000 Zagreb
E-mail: zdenko.kovacic@fer.hr
URL: http://aus-www.rasip.fer.hr/kovacic/index.html

Received: 2002–07–12